Electronic Supplementary Material (ESI) for Journal of Materials Chemistry A.

Supporting Information

Ultrathin Insulating Under-Layer of Hematite Thin Film for Enahnced Photoelectrochemical (PEC) Water Splitting Activity

Myung Jong Kang and Young Soo Kang *

Korea Center for Artificial Photosynthesis and Department of Chemistry, Sogang University, Seoul, 121-742, Korea.

E-mail: yskang@sogang.ac.kr

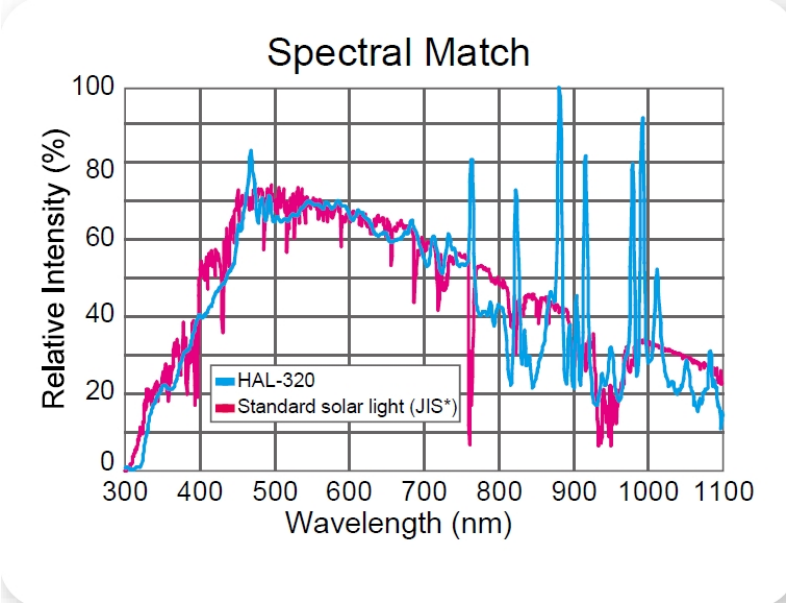

Figure S1. Spectral Match data of 1 sun light source (HAL-320, Asahi spectra, Japan) compared with standard solar light (JIS certified). (300 ~ 1100 nm, with AM (air mass) 1.5 filtered).[s1]

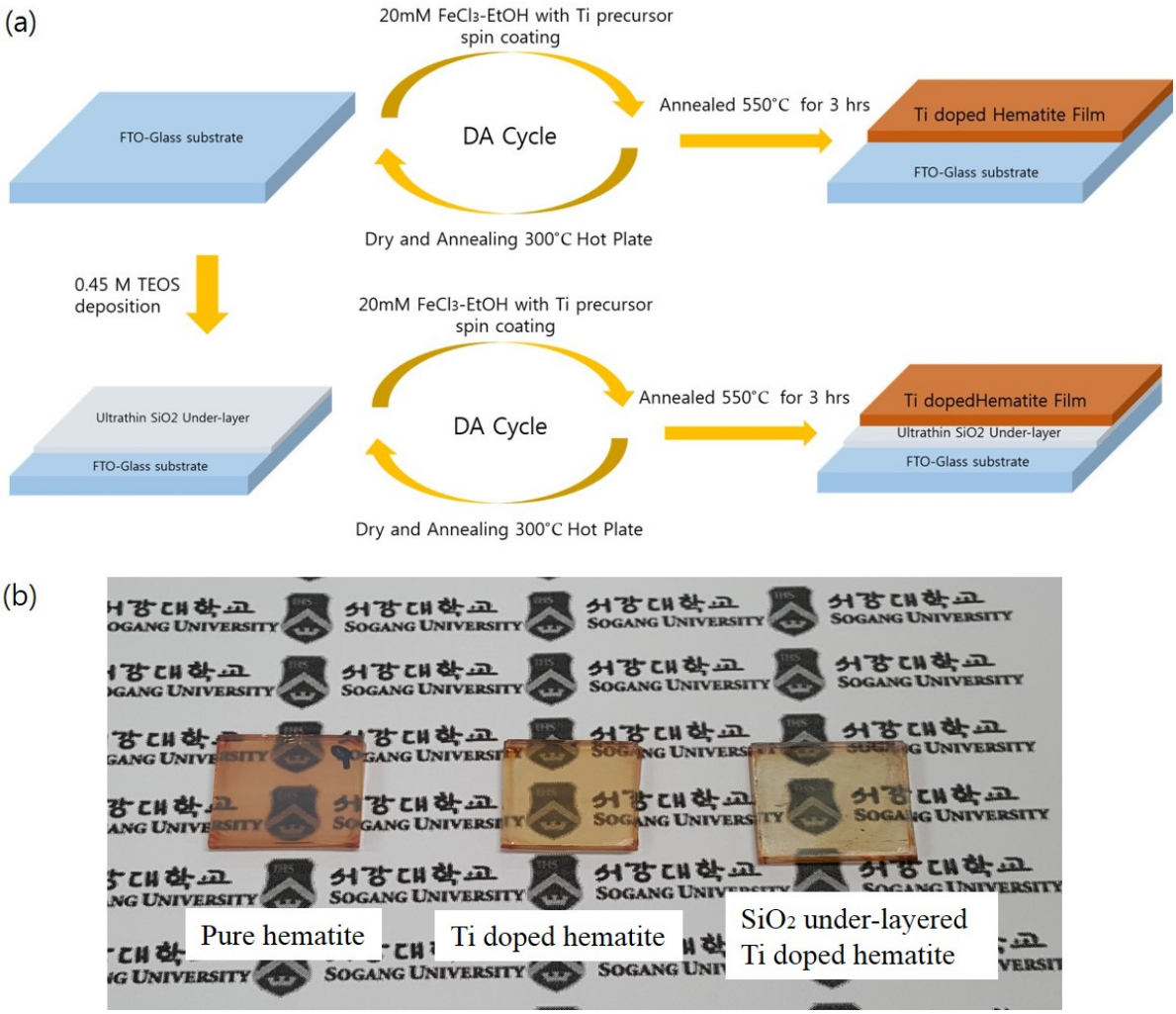

Figure S2. (a) Schematic drawings for fabrication Ti doped hematite film and ultrathin SiO_2 under-layered Ti doped hematite film. (b) optical images of pure hematite film, Ti doped hematite film and SiO_2 under-layered Ti doped hematite film.

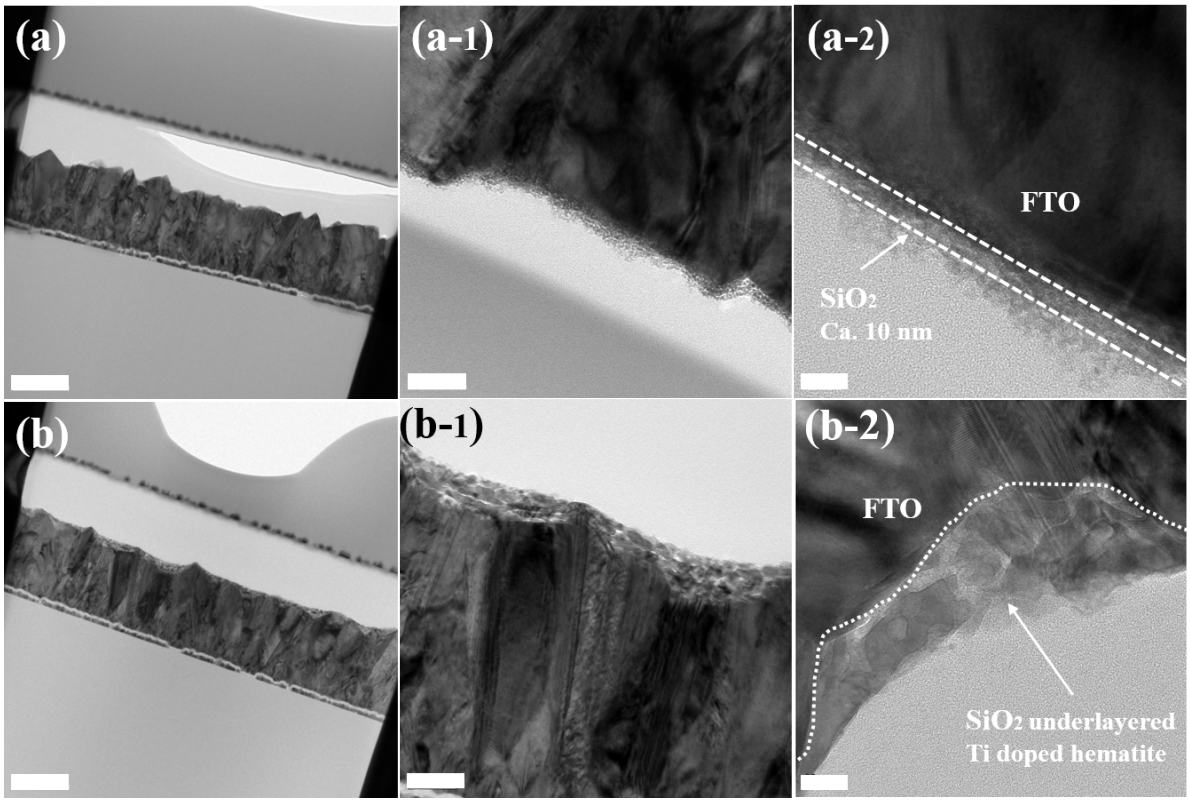

FigureS3. TEM images of 3 times deposited SiO_2 under-layer (a, a-1, a-2) and 1 time deposited SiO_2 under-layered Ti doped hematite film (b, b-1, b-2). (The scale bar is 0.5 μm, 100 nm and 20 nm, respectively)

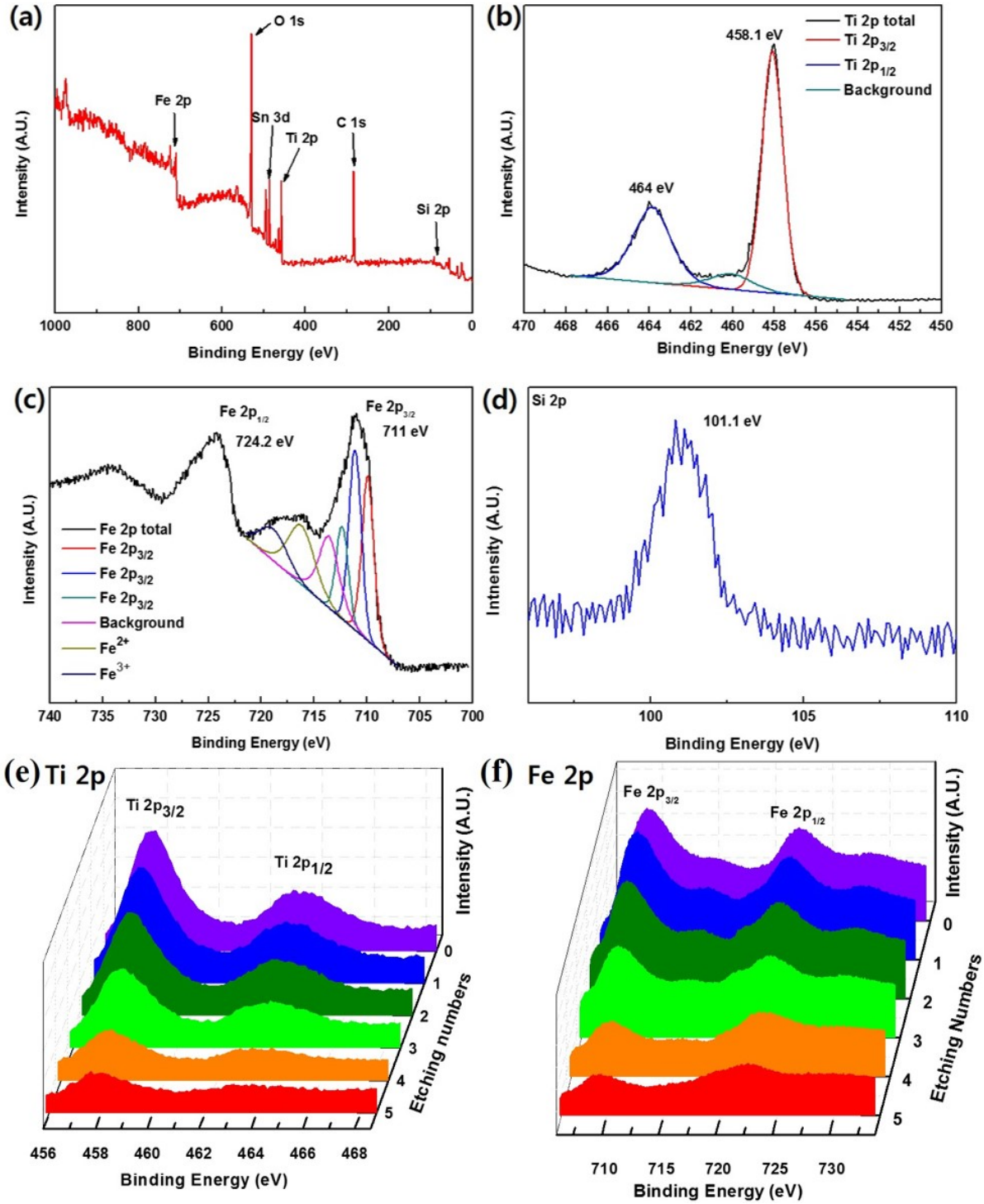

Figure S4. XPS data of SiO_2 under-layered Ti doped hematite film. (a) survey scan, (b) Ti 2p, (c) Fe 2p and (d) Si 2p. Depth profiling of (e) Ti 2p, (f) Fe 2p in SiO_2 under-layered Ti doped hematite film.

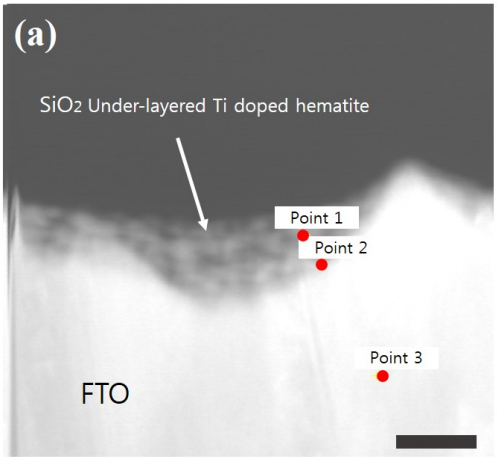

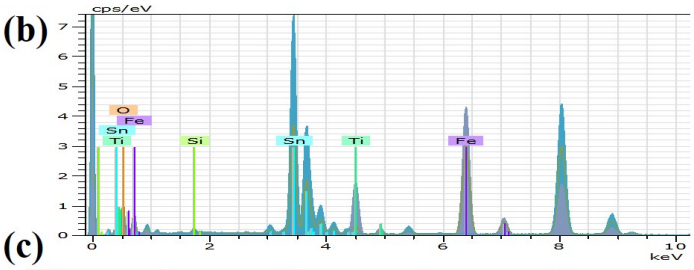

(c)

Atom.%	Si	Ti	Fe	Sn
Point 1	0.39	20.80	57.21	0.47
Point 2	0.67	1.74	26.91	65.56
Point 3	0.25	0.00	0.10	97.08

Figure S5. TEM EDXS point analysis of SiO_2 under-layered Ti doped hematite film. (a) STEM image for position of points, (b) acquired spectrum, (c) Table of atomic percentage for Si, Ti, Fe and Sn. (point 1 for hematite film, point 2 for interface between hematite and FTO substrate and point 3 for inside of FTO substrate).

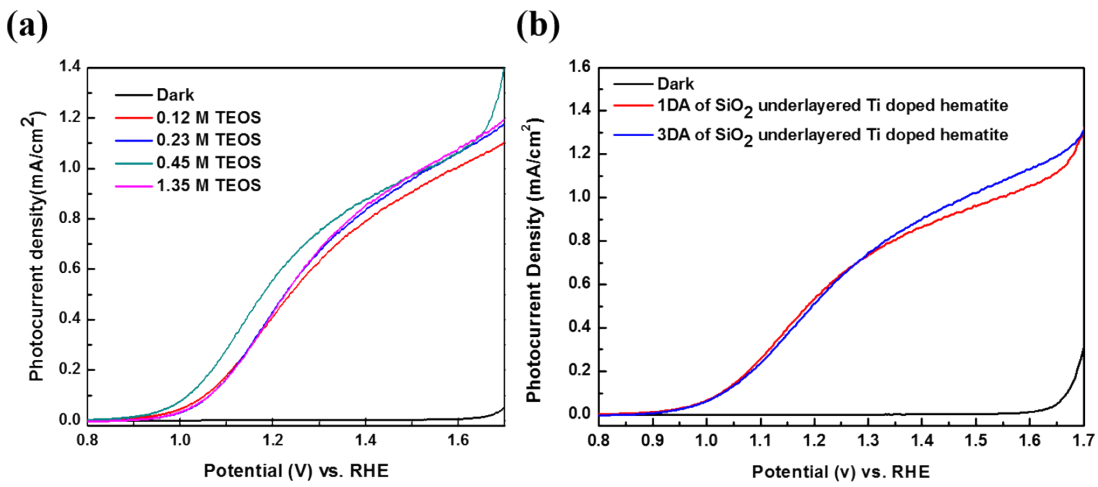

Figure S6. Photocurrent density curves of SiO_2 under-layered Ti doped hematite film with (a) different Si precursor concentration for SiO_2 under-layer (1 time deposited) and (b) different DA cycle number of SiO_2 under-layer with 0.45 M of Si precursor.

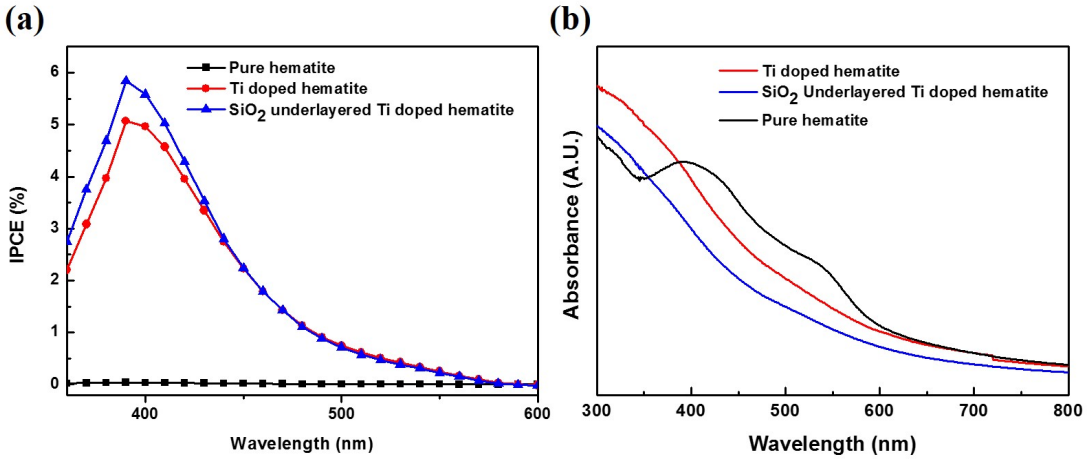

Figure S7. (a) Incident photon to current conversion efficiency (IPCE) curve and (b) UV-Vis spectrum for pure hematite, Ti doped hematite and SiO_2 under-layered Ti doped hematite film.

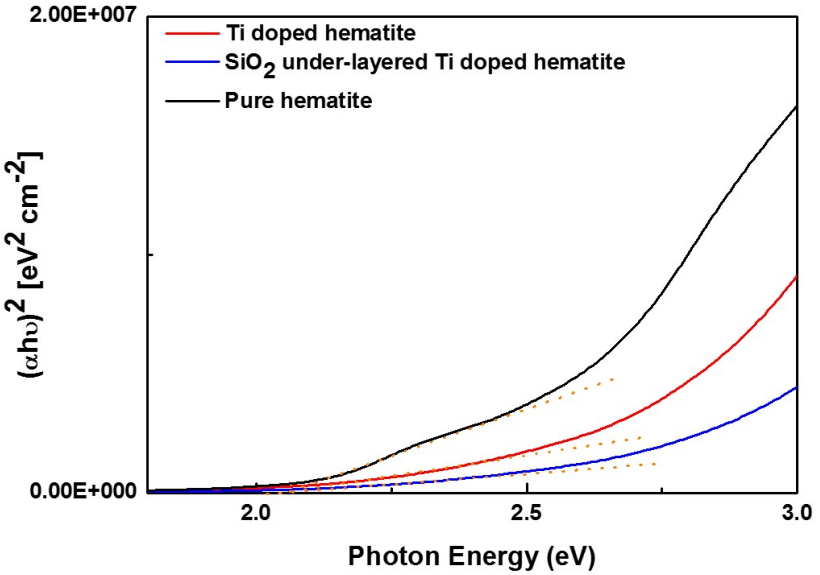

Figure S8. Tauc plot for pure hematite, Ti doped hematite and SiO_2 under-layered Ti doped hematite film.

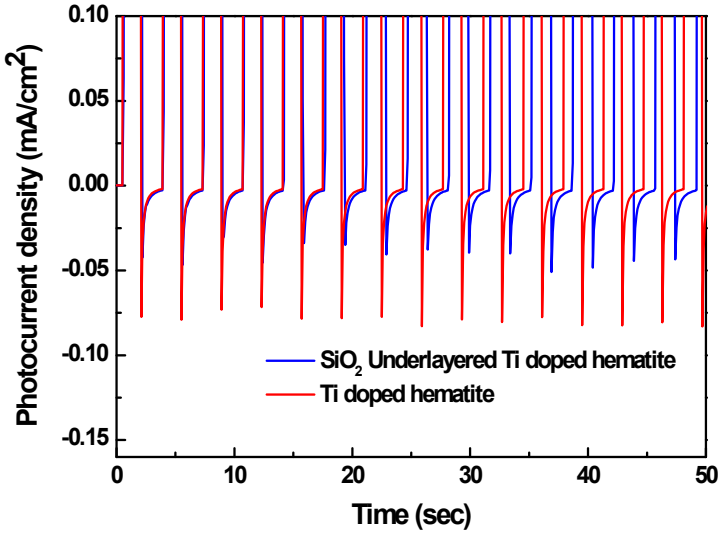

Figure S9. Reverse current magnified transient J-V curve for Ti doped hematite and SiO_2 under-layered Ti doped hematite film (1.23 V vs. RHE potential applied).

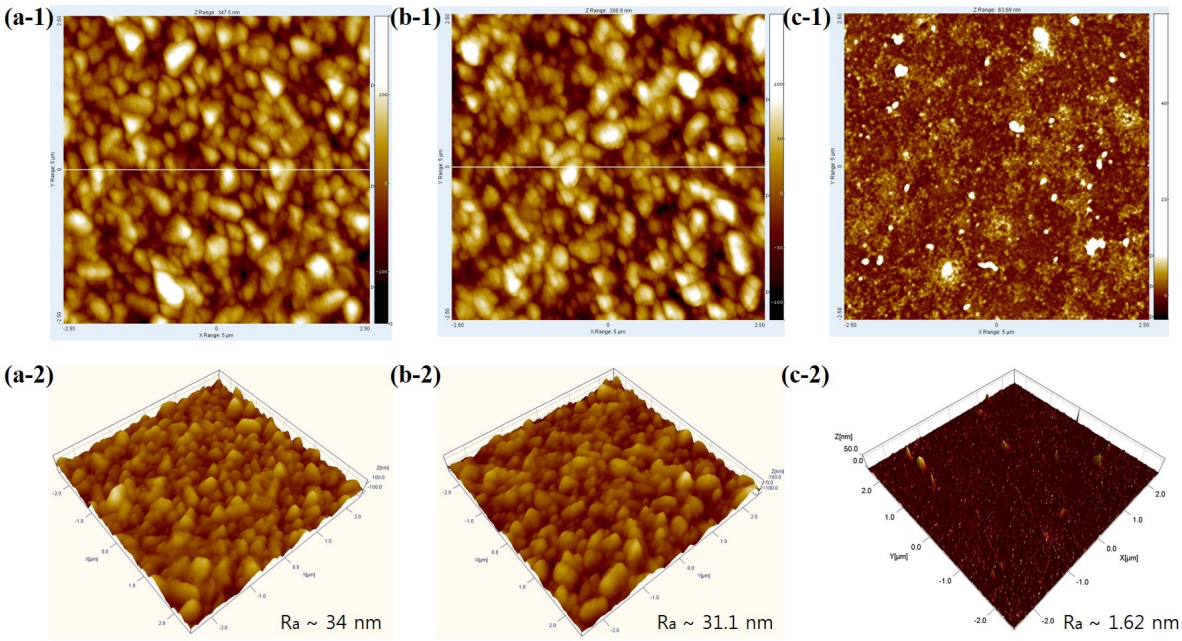

Figrue S10. AFM images and 3-D topography of pure hematite film (a-1, a-2), Ti doped hematite film (b-1,b-2) and SiO_2 under-layered Ti doped hematite film (c-1, c-2), respectively (all scales are 5 μm by 5 μm).

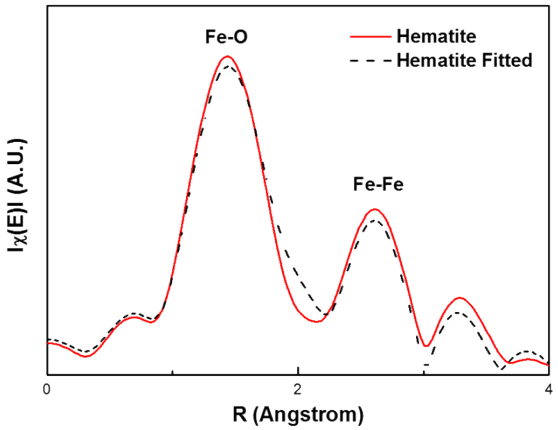

Figure S11. Refined EXAFS spectrum of pure hematite with furrier transformed in R space and fitted with ifeffit algorithm-based calculation.

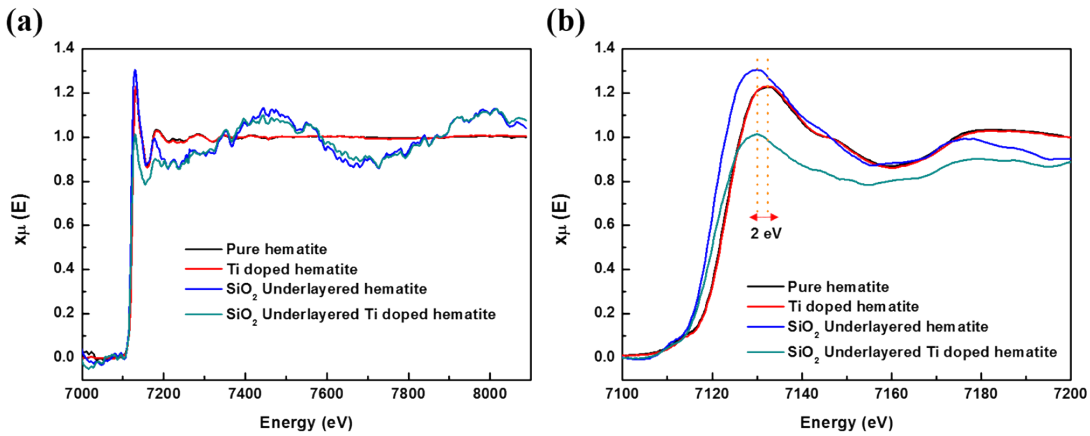

Figure S12. (a) X-ray absorption fine structure (XAFS) spectra and (b) X-ray absorption near edge spectra (XANES) for pure hematite, Ti doped hematite, SiO_2 under-layered hematite and SiO_2 under-layered Ti doped hematite film.

Reference for Supporting Information

[S1] The Asahi-spectra USA online, http://www.asahi-spectra.com/opticalinstrument/hal320.html, (accessed June 2015).